https://doi.org/10.3311/PPee.20140



**Periodica Polytechnica Electrical Engineering and Computer Science**, 66(4), pp. 315–324, 2022

# Optimization of Photovoltaic Water Pumping System Based on BLDC Motor for Agricultural Irrigation with Different MPPT Methods

Fatima Belgacem[1*], Mohamed Mostefai[2], Miloud Yahia[2], Aicha Belgacem[1]

[1] Laboratoire Génie Electrotechnique, Department of Electrical Engineering, Faculty of Technology, University Dr Moulay Tahar of Saida, 20000 Ennasr, Saida, P.O.B. 138, Algeria
[2] Laboratoire Géométrie, Analyse, Contrôle Et Applications, Department of Electrical Engineering, Faculty of Technology, University Dr Moulay Tahar of Saida, 20000 Ennasr, Saida, P.O.B. 138, Algeria
[*] Corresponding author, e-mail: fatima.belgacem@univ-saida.dz

Received: 11 March 2022, Accepted: 20 September 2022, Published online: 03 October 2022

**Abstract**

This study presents a comparative analysis of different MPPT techniques for PV array fed water pumping system without batteries using brushless direct current (BLDC) Motor. The system is configured to reduce both cost and complexity with simultaneous assurance of optimum power utilization of PV array, for this we propose two intelligent maximum power point tracking MPPT techniques implemented through a boost converter; the first is based on Fuzzy Logic Controller (FLC) the second is a sliding mode control, which have been successfully applied to Photovoltaic Pumping System (PVPS) to replace tracking power point perturb and observe (P&O) under different conditions of solar radiation. As a result, the PV must be turned on at its highest power extracted. The water pumping system is designed to irrigate an area of 8 hectares, planted with onions, we have chosen a BLDC motor which is coupled with a centrifugal pump to overcome the disadvantage of brushed motors and induction motors. The object is to verify and confirm the effectiveness of the suggested system. According to simulation data, FLC improves the PVPS's performance.

**Keywords**

photovoltaic pumping system, agricultural irrigation, brushless DC motor, fuzzy logic control, sliding mode control

## 1 Introduction

Over the past few years, the world has experienced a significant growth in demand for energy in all areas of life, in particular electricity which unfortunately comes largely from fossil energy sources, which have a very harmful impact on the environment. The solution is based on the use of renewable energies. in this context, many countries have made huge investments and thus seem to be on the right track to meet the challenge of combining energy production and consumption on the one hand and maintaining the ecological balance of the planet on the other hand. The sun in this case remains, directly or indirectly, the most promising energy source [1].

Stand-alone pumping systems powered by electrical motors are the most common application of photovoltaic energy in Algeria [2]. Indeed, it is the most widely used energy source for providing drinking and irrigation water in rural areas that cannot afford to connect to the national grid. The major part of the pumping systems currently implemented as electric actuator using the direct current (DC) motor, brushless motor BLDC or induction motor. However, Induction motors are not really suitable for PVPS because they are prone to overheating if the voltage is too low and require extensive control [3]. Because of its longer operational life, higher dependability, noiseless performance, high efficiency, ability to run at low voltage, high torque/weight ratio, easy-to-drive features, and great performance over a wide speed range, the BLDC is chosen to drive the proposed system [3, 4].

Solar energy has the benefit of being both free and unlimited, however photovoltaic panels, like other renewable energy sources, offer very variable energy and are heavily dependent on weather circumstance. MPPT algorithms make it possible to obtain the best power output of the panel. they allow Photovoltaic (PV) system to work at maximum power points of their characteristics without prior knowledge of these operating points and their variation following changing weather conditions [5].

**Cite this article as:** Belgacem, F., Mostefai, M., Yahia, M., Belgacem, A. "Optimization of Photovoltaic Water Pumping System Based on BLDC Motor for Agricultural Irrigation with Different MPPT Methods", Periodica Polytechnica Electrical Engineering and Computer Science, 66(4), pp. 315–324, 2022. https://doi.org/10.3311/PPee.20140

In the literary works, there are many MPPT strategies based on methods such as Zarour et al. [6] proposed a sliding mode controller (SMC) for the photovoltaic pumping system(PVPS) to optimize the photovoltaic generator in order to provide maximum power, and Rekioua et al. [7] applied a sliding mode control for the same goal. While Abderrahim et al. [8] presents an improved MPPT methods for a PV system under a variety of climatic situations, the first is a sliding mode MPPT, the second MPPT is based on the incremental conductance algorithm. It gives the SMC the reference PV voltage. Otherwise, Hasan et al. [9] proposed fuzzy rule for MPPT provide the pulse for the zeta converter to drive the brushless DC motor in water Pumping system, it is efficient smart control to extract optimal power from the generator photovoltaic (GPV) and boosts the speed in order to keep track of the maximum power output.

The main goal of this study is the employment of FLC and SMC techniques for PV system of a standalone photovoltaic system fed brushless DC motor with a centrifugal pump to meet the irrigation needs of onion farming. In order to demonstrate the efficacy of the proposed strategy a comparison of the P&O, SMC, and FLC MPPT methods will be studied for the tracking of the point of maximum power provided to the pumping system.

In a first step, a pumping system design, as well as its architecture and its design is presented. A precise outline on the regulators and the converters is carried out. The second step is devoted to the pumping system control where the description of MPPT methods, and the electronic commutation for BLDC motor are presented. Then, results of simulations for the entire system are presented, carried out with the Matlab®/Simulink software, with the chosen methods the P&O, FLC and SMC under sudden change in solar irradiation and under autumn and summer day irradiation.

## 2 Design of pumping system

The agricultural land specifications are presented in Table 1.

**Table 1** Agricultural land specifications

| Symbol | Designation |
|---|---|
| $Q$ | Flow rate the of the pumping is 20 m$^3$ per hour |
| $T_{pum}$ | Daily functioning time is 6 h |
| $H_{mt}$ | Manomeric height is 10 mca |
| $C_h$ | Hydraulic constant |
| $\eta$ | Efficiency of moto-pump |
| $V_{tank}$ | The volume tank is 120 m$^3$ |

### 2.1 Case study

The water pumping system is designed to irrigate an area of 8 hectares of onion farming, this area was divided into five parts, each of them being irrigated for 6 hours per five days from 10 am to 4 pm which is an opportunity not to use an energy storage (Pumping over sun).

A schematic representation of the pumping system is shown in Fig. 1, where it describes the components of pumping systems.

Solar energy will be captured by means of photovoltaic panels and converted into electricity [10], which will power the BLDC motor and will turn on the water pump that will pump the water from a well with depth of 10 m to the tank. The architecture of the entire system is described in Fig. 2.

The GPV energizes the BLDC motor with maximum power through several MPPT control to choose a best one in order to drive the motor optimally, according to the maximum power. This MPPT is integrated into the boost converter, which in turn feeds the voltage source

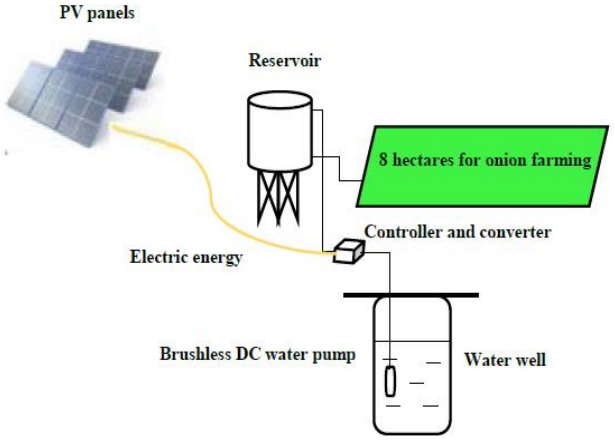


**Fig. 1** Schematic representation of the PVP system

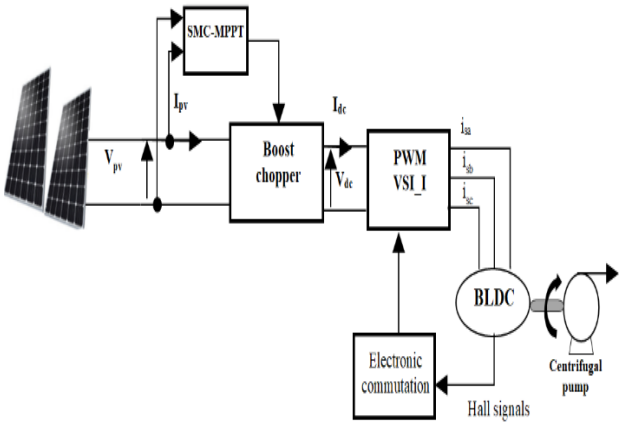


**Fig. 2** The proposed system architecture

inverter (VSI) supplying the BLDC motor coupled with the centrifugal pump. As for the motor control side, the electronic commutation is preferred, it is the process of a BLDC motor's inbuilt encoder decoding hall effect signals depending the rotor position, and provides Switching sequence to the VSI.

The suggested system is constructed in such a way that it always performs satisfactorily regardless of the quantity insolation, as follows.

### 2.2 GPV design

The electric power required by the pump was determined by [11]:

$$P_e = \frac{C_h \cdot Q \cdot H_{mt}}{\eta}. \tag{1}$$

The hydraulic constant is calculated by Eq. (2):

$$C_h = \frac{g \cdot \rho}{3600}. \tag{2}$$

For sizing the photovoltaic generator, it is necessary to calculate the electrical energy $E_{el}$ consumed during pumping time in a day [12] it can be calculated by:

$$E_{el} = P_e \cdot T_{pum}. \tag{3}$$

The pumping time $T_{pum}$ can be calculated by:

$$T_{pum} = \frac{V_{\text{tank}}}{Q}. \tag{4}$$

The energy produced by a photovoltaic field $E_p$ is equal to:

$$E_P = \frac{E_{el}}{K}, \tag{5}$$

where $K$ is the correction coefficient depending on the meteorological uncertainty, the inclination of the solar modules and the overall efficiency of the photovoltaic system [13].

The peak power of the photovoltaic generator $P_c$ is calculated as follows:

$$P_c = \frac{E_p}{G}, \tag{6}$$

where $G$ is the average daily irradiation.

The total number of photovoltaic modules $N_{Tot}$ is calculated by relating the overall power of the field $P_{PV}$ to that $P_{\text{mod}}$ of a single module:

$$N_{Tot} = \frac{P_{PV}}{P_{\text{mod}}}. \tag{7}$$

Table 2 summarizes the sizing results. Two modules are connected in parallel and five modules are joined in series to make a 1.9 kW PV array that will feed a 1.3 kW BLDC. The slightly overrated PV array is selected to meet the desired requirement and losses incurred in the system. The detailed specifications of PV array are given in Table 3.

### 2.3 Design of boost converter

The PV array voltage ($V_{pv}$) and DC link voltage ($V_{\text{DC}}$) are respectively 150 V and 360 V.The boost duty ratio and the DC current are provided in Eq. (8) and Eq. (9). Supposed the boost converter ideality [14].

$$D = 1 - \frac{V_{PV}}{V_{\text{DC}}} \tag{8}$$

$$I_{\text{DC}} = \frac{P_{pv}}{V_{\text{DC}}} \tag{9}$$

The inductance $L_{\min}$ and capacitance $C_{\min}$ are calculated from Eq. (10) and Eq. (11), also the converter is considering lossless [14]:

$$L_{\min} = \frac{DV_{pv}}{f_s \Delta I_L}, \tag{10}$$

$$C_{\min} = \frac{10 \cdot I_{\text{DC}}}{\pi N \cdot N_p \cdot \Delta V_{\text{DC}}}. \tag{11}$$

The boost parameters are shown in Appendix (Table A1).

**Table 2** Dimensioning results

| | |
|---|---|
| Efficiency of moto-pump (%) | 52.25 |
| Electric power required by the pump $P_e$ (W) | 1043 |
| Electrical energy $E_{el}$ (Wh/j) | 6258 |
| Energy produced by a photovoltaic field $E_p$ (Wh/j) | 10430 |
| The peak power of the PVG $P_c$ (W) | 1738.33 |
| Photovoltaic modules number $N_{Tot}$ | 10 |

**Table 3** Photovoltaic panel "DIMEL solaire" parameters

| Electrical characteristics | Values |
|---|---|
| Maximum power ($P_{\max}$) | 190 W |
| Voltage at $P_{\max}$ ($V_{mp}$) | 30.4 V |
| Current at $P_{\max}$ ($I_{mp}$) | 6.25 V |
| Open-circuit voltage ($V_{oc}$) | 36.2 V |
| Short-circuit current ($I_{sc}$) | 6.7 A |
| Size | 1640 × 992 × 35 mm |
| Weight | 17.79 Kg |
| Cells | 60 Pcs, 156 × 156 Monocrystalline Silicon |

### 2.4 Water pump design

The power consumption of a water pump is proportional to its speed cubed.

The pump proportionality constant $K_p$ can be calculated for an input power and rated speed of 1.3 KW and 2500 rpm, respectively [15]:

$$K_p = \frac{P}{(\pi / 30 \times N)^3} = 0.00007 \ \ \sec^3 / \mathrm{rad}^3, \tag{12}$$

where $P$ is the input power of the BLDC motor.

## 3 Control and operation

In Section 3, the system's controls are presented, starting by MPPT control, then the BLDC electronic commutation are detailed.

### 3.1 Maximum power point tracking

Section 3.1 is devoted to the description of SMC and P&O MPPT algorithm in order to obtain the generator's maximum power.

#### 3.1.1 Perturbation and observation (P&O)

Because its algorithm is simple to implement, the P&O approach is the most widely used in the industrial context. This approach works by causing a disturbance in the system by increasing or decreasing the operational voltage of the module and evaluating the effect on the array's output power. Fig. 3 shows the flowchart of the P&O method algorithm [16].

#### 3.1.2 The sliding mode control

For this method, P&O MPPT controller was replaced by SMC. The most important step in SMC is specifying the sliding surface, the choice of the latter depends on obtaining the maximum amount of energy from the PV array, the sliding mode control function is to track the maximum power point by changing the duty cycle of the boost converter.

Thus, the SMC design can be created in two parts [4]:

- The sliding surface selection:
  - The sliding surface is formulated as having:

$$\delta = \frac{\Delta P_{pv}}{\Delta V_{pv}} = 0. \tag{13}$$

- Define the control law, Eq. (13) becomes:

$$\delta = \frac{\Delta P_{pv}}{\Delta V_{pv}} = \frac{\Delta I_{pv}^2 R_{pv}}{\Delta V_{pv}} = I_{pv} + V_{pv} \frac{\Delta I_{pv}}{\Delta V_{pv}} = 0. \tag{14}$$

The SMC structure has two parts: the first is the equivalent control quantity $U_{eq}$, which keeps the operation point in the switching surface and removes it to the origin, and the second is $U_n$, which offers controller stability, where:

$$u = u_{eq} + u_n, \tag{15}$$

with:

$$u_{eq} = 1 - \frac{V_{pv}}{V_{\mathrm{DC}}}, \tag{16}$$

and:

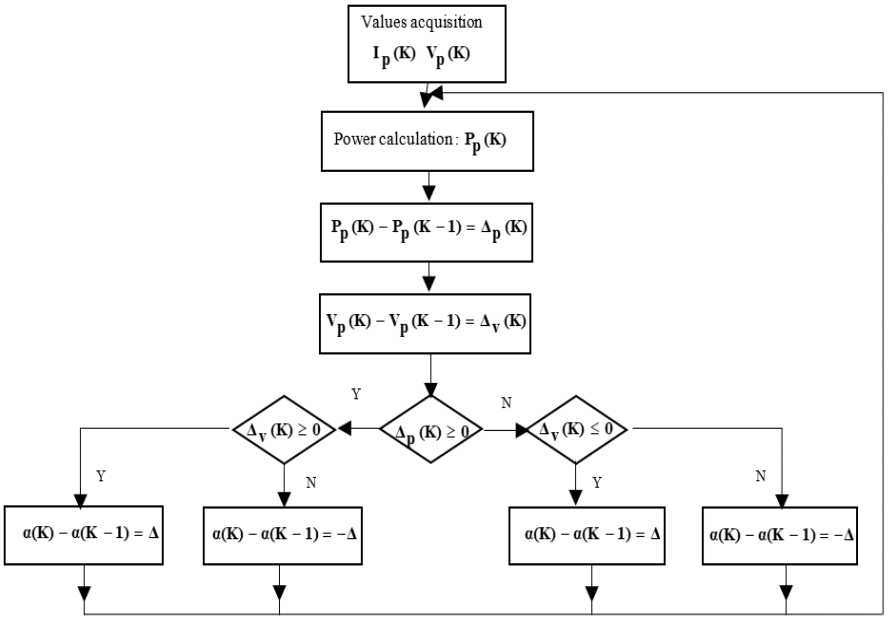


**Fig. 3** Flowchart of perturbation & observation MPPT algorithm

$$u_n = \lambda \cdot \mathrm{sgn}(\delta), \tag{17}$$

where $\lambda$ is a positive constant.

The Lyapunov method is used to determine the current system stability as:

$$V = \frac{1}{2}\delta^2. \tag{18}$$

The reachability criteria to achieve the sliding surface in sliding mode dynamics is specified in Eq. (19) to ensure control stability.

$$\dot{V} = \delta \cdot \dot{\delta} < 0 \tag{19}$$

As a result, it is demonstrated that the system adheres to the stability criterion even when characteristics such as sun irradiation fluctuate.

### 3.1.3 Fuzzy logic controller

Fuzzy logic techniques are applied to construct the MPPT controller for GPV. The FLC determines the optimal duty cycle for feeding the converter's switch [17]. Fuzzification, inference are the processes of the MPPT controller technique employing FLC algorithm as well as the defuzzification. The following diagram depicts the fuzzy controller's basic construction (Fig. 4) [18, 19]:

Table 5 presents the FLC rules, where (Ɛ(k)), (DƐ(k)) and (D) are the inputs of the matrix, with Ɛ(k) is fuzzy sets of error, DƐ(k) is change of error and D is change of duty cycle at the boost.

In the case of FLC, the rules of the control must be designed in such a way that the input Ɛ(k) is always zero.

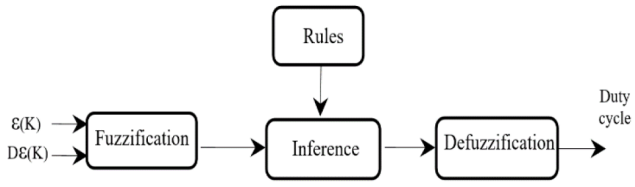


**Fig. 4** A fuzzy controller's basic schematic diagram

**Table 5** Table of rules of five class (inference matrix)

| Ɛ(k) | DƐ(k) | | | | |
|---|---|---|---|---|---|
| | NB | NS | ZE | PS | PB |
| NB | ZE | ZE | PB | PB | PB |
| NS | ZE | ZE | PB | PB | PB |
| ZE | PS | ZE | ZE | ZE | NS |
| PS | NS | NS | NS | ZE | ZE |
| PB | NB | NB | NB | ZE | ZE |

Where the FLC rules are defined as NB, NS, ZE, PS, and PB stand for Negative Big, Negative Small, Zero, Positive Small, and Positive Big, respectively.

### 3.2 Electronic commutation

The BLDC electronic commutation generates the switching signals for the VSI [20, 21]. The encoder generates three Hall Effect signals based on the rotor's angular position, which are utilized to feed the VSI's six switches, as indicated in Table 6 [3].

## 4 Simulation results and comparative study

MATLAB/Simulink software is used to run various tests to evaluate the success and robustness of the suggested control. At the beginning, we apply a sudden change in irradiation as shown in Fig. 5; a sunlight level of 0.6 kW/m² is applied after 5 seconds, it is varied to 1 kW/m² and at 8 second the irradiation level is 0.8 kW/m² while the temperature is kept at 25 °C. results are illustrated in Fig. 6 and Fig. 7.

The power response of PV array is shown in Fig. 6 using three MPPT strategies. The PV power controlled by SMC quickly reach the steady state with high values compared

**Table 6** Switching states for BLDC motor electronic communication

| | Hall signals | | | Switching states | | | | | |
|---|---|---|---|---|---|---|---|---|---|
| θ, deg | $H_3$ | $H_2$ | $H_1$ | $S_1$ | $S_2$ | $S_3$ | $S_4$ | $S_5$ | $S_6$ |
| NA | 0 | 0 | 0 | 0 | 0 | 0 | 0 | 0 | 0 |
| 0–60 | 1 | 0 | 1 | 1 | 0 | 0 | 1 | 0 | 0 |
| 60–120 | 0 | 0 | 1 | 1 | 0 | 0 | 0 | 0 | 1 |
| 120–180 | 0 | 1 | 1 | 0 | 0 | 1 | 0 | 0 | 1 |
| 180–240 | 0 | 1 | 0 | 0 | 1 | 1 | 0 | 0 | 0 |
| 240–300 | 1 | 1 | 0 | 0 | 1 | 0 | 0 | 1 | 0 |
| 300–360 | 1 | 0 | 0 | 0 | 0 | 0 | 1 | 1 | 0 |
| NA | 1 | 1 | 1 | 0 | 0 | 0 | 0 | 0 | 0 |

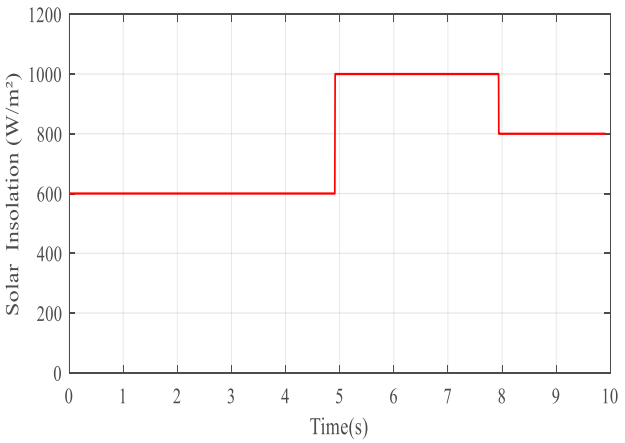


**Fig. 5** Solar insolation level

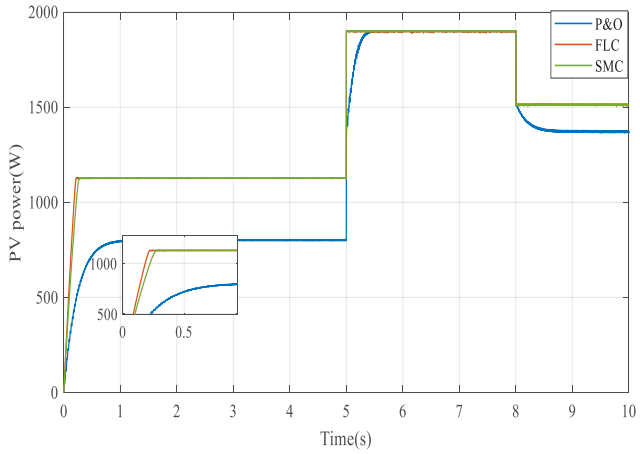


**Fig. 6** Power response of GPV

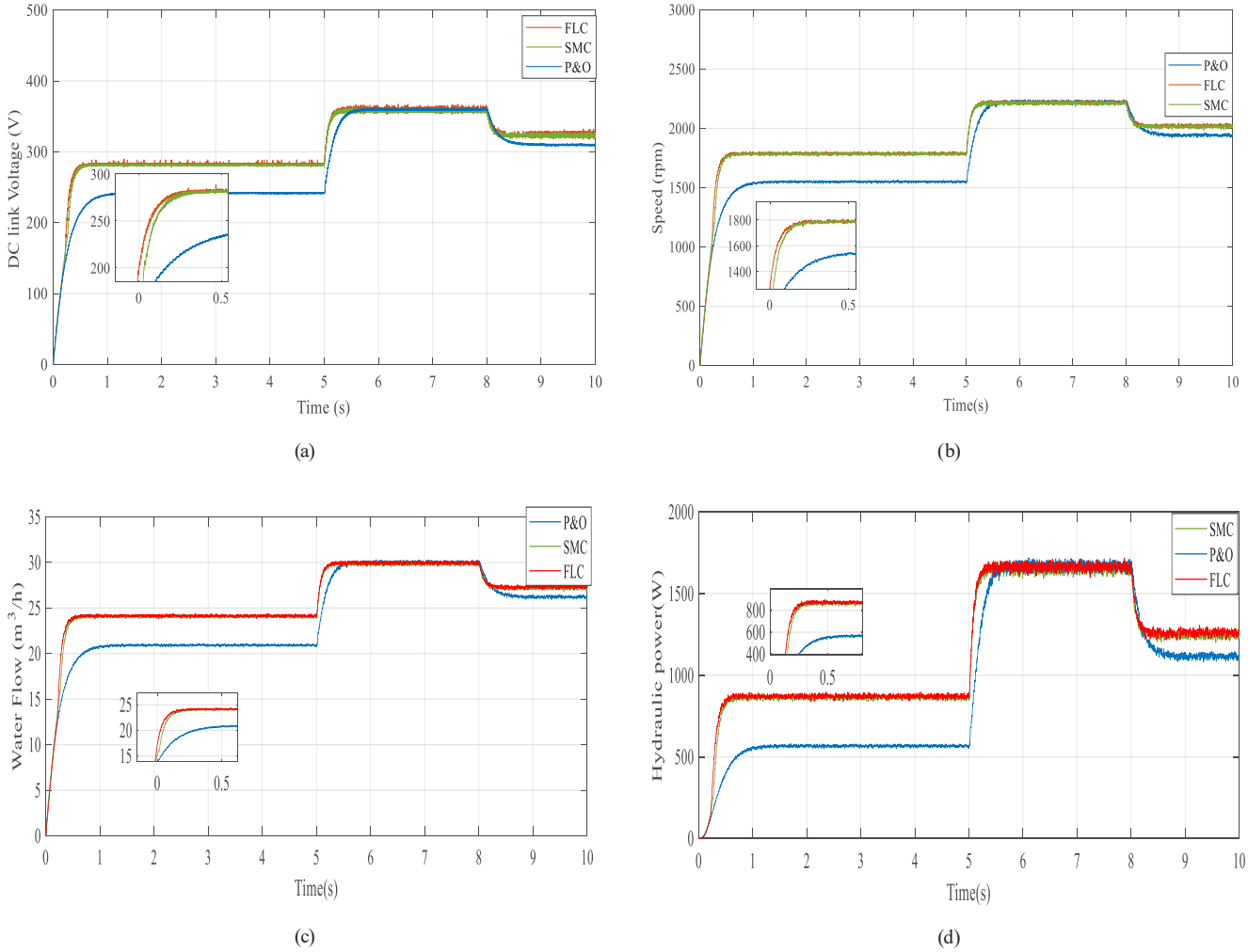


**Fig. 7** Response of motor-pump; (a) DC link voltage; (b) Speed; (c) Flow rate; (d) Hydraulic power

to the PV system controlled by P&O. As for the FLC control, it is faster than the two mentioned. Despite weather changes, the PV generator is forced to function at its maximum power point by FLC and SMC MPPT methods.

As it can be noticed from Fig. 7 that the variation of the insolation affects the motor-pump parameters, it is also shown in Fig. 7(a), (b) and (c) the DC link voltage, the speed response and water flow respectively while Fig. 7(d)

shows the hydraulic power. The motor-pump parameters with SMC are fast and higher than those with P&O, while the FLC control is faster than the previous controls.

We can conclude that our proposed method is more efficient and this is shown in the PV power response, the water flow and the hydraulic power.

All these results clearly show the superiority and efficiency of the proposed FLC and SMC controller compared to P&O. Moreover, there are an obvious quick response on the curve of the FLC controller which proves its stability and good performance.

In order to ensure that the suggested control is successful, it is preferred to develop a full simulation model of the proposed PVPS configuration under real data climate conditions of a day of December (Fig. 8) and another day of August (Fig. 9) in northwest Algeria [22]. The results are shown as follow:

Fig. 10 presents comparative results of the three controllers during a December day, where it is clear in Fig. 10(a) that the GPV power with FLC and SMC method is higher

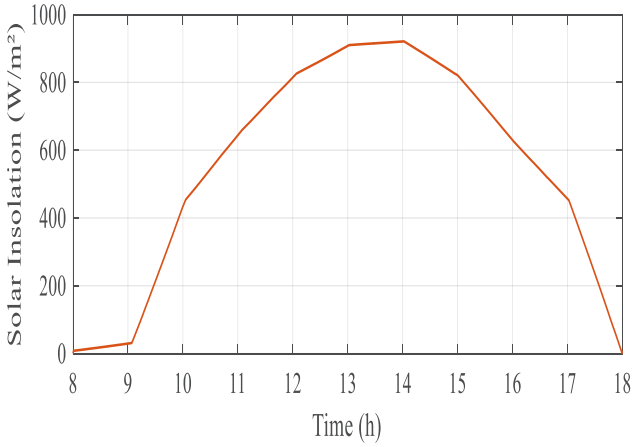


**Fig. 8** Solar irradiation for a day of December

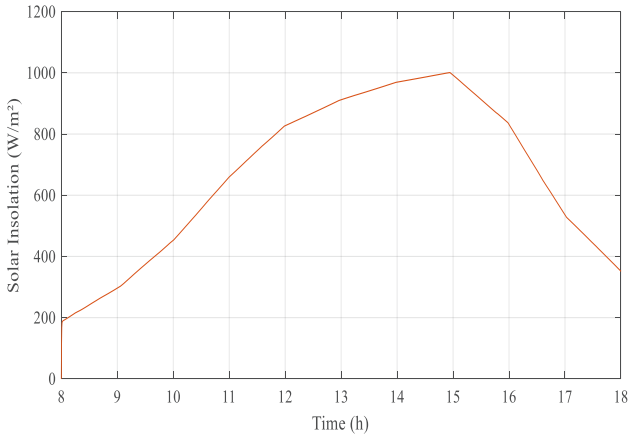


**Fig. 9** Solar irradiation for an August day

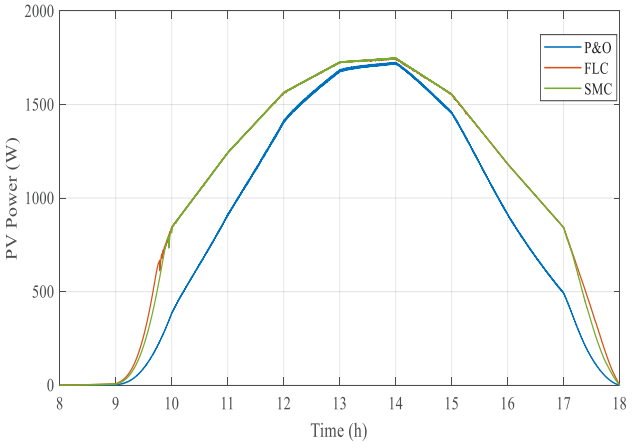


(a)

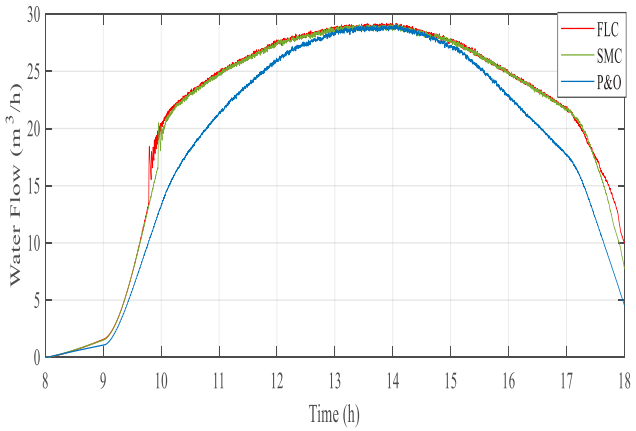


(b)

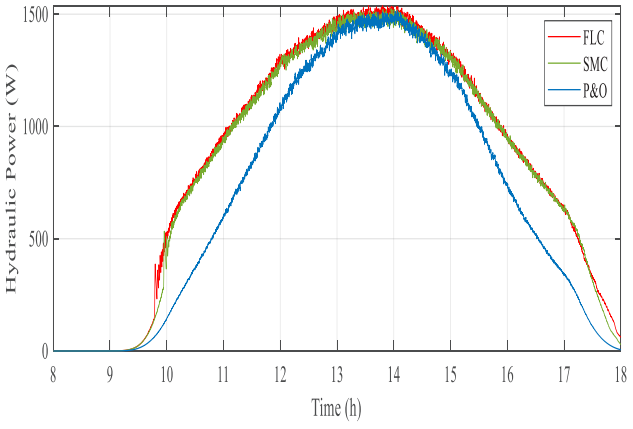


(c)

**Fig. 10** Comparison of PVPS response utilizing three controllers for a December day; (a) GPV power; (b) Water pump flow; (c) Hydraulic power

than that with P&O. Fig. 10(b) and Fig. 10(c) show the water flow and the hydraulic power respectively where it is also noted the superiority of the FLC method. The same note concerning the results of the three controllers during

an august day where Fig. 11(a) shows the GPV power, Fig. 11(b) shows the water flow pump and Fig. 11(c) shows the hydraulic power.

From Fig. 10 and Fig. 11, it is noted that at sunrise and at sunset, both methods FLC and SMC are higher than P&O with a small delay in SMC compared to FLC, However, during the middle of the day, when big amounts of water are required, all controllers work fine.

As it can be seen in Fig. 12, When the FLC and SMC are used, the pumped volume is clearly greater than when the conventional method is used, with slight elevation of FLC technique.

Once again, the proposed FLC control proves its effectiveness by showing better results than SMC and P&O under real data climate conditions of both autumn and summer day.

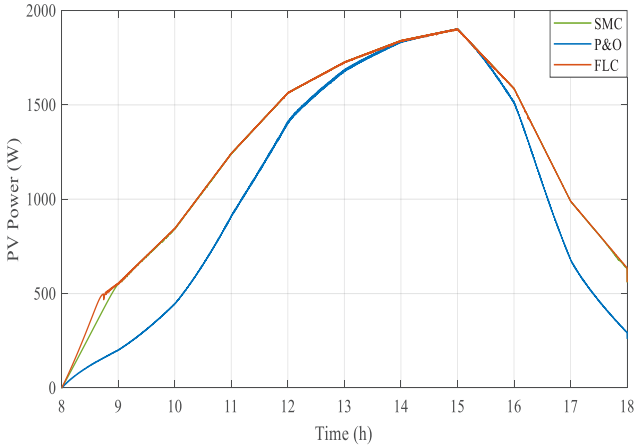


(a)

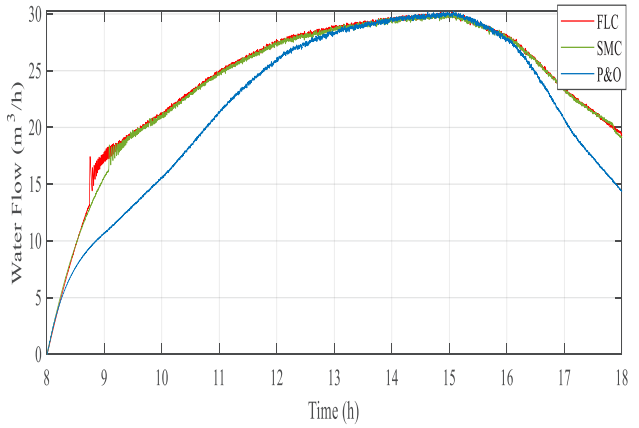


(b)

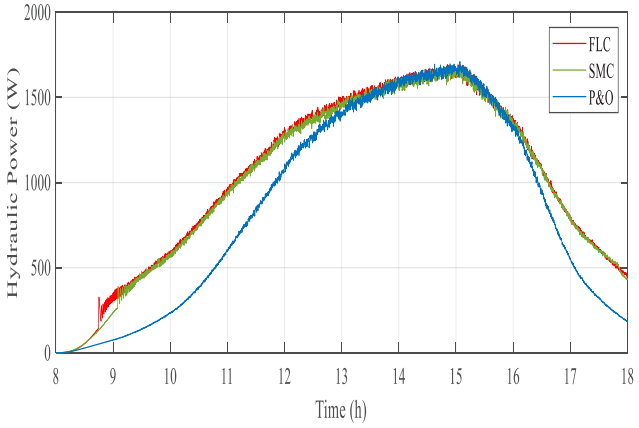


(c)

**Fig. 11** Comparison of PVPS response utilizing three controllers for an August day, (a) GPV power; (b) Water pump flow; (c) Hydraulic power

## 5 Conclusion

The aim of this paper is to present a comparative analysis of different MPPT techniques for solar water pumping system without batteries using BLDC Motor in order to meet the irrigation of 8 hectares of agriculture land of onion farming.

A proposed control with FLC and SMC based MPPT is presented. MATLAB and its Simulink have been used to develop and simulate the proposed system. The simulation findings verify the system's design and performance, demonstrating that FLC and SMC, when compared to P&O, produce more reliable results in terms of good tracking, stability, and fast response time under variable solar irradiations while the FLC has proven its worth in the quick PVPS response which improves the efficiency of PVPS. This last allows the irrigation of the agricultural land successfully and satisfactorily.

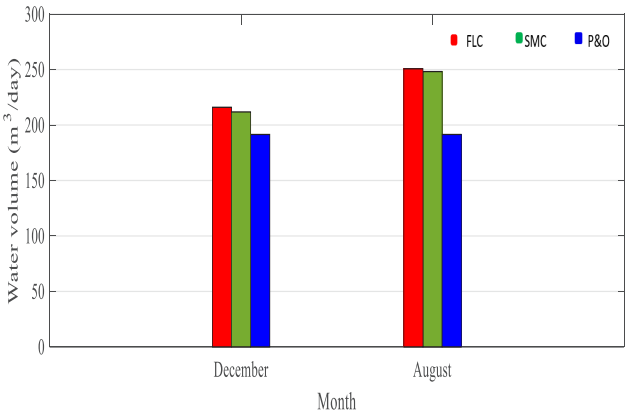


**Fig. 12** Comparative histogram of water volume

## References

[1] Boukebbous, S., Kerdoun, D., Benbaha, N., Ammar, H., Boutadara, A. "Effet de l'ombrage sur un systeme de pompage photovoltaique" (Effect of shading on a photovoltaic pumping system), International Journal of Scientific Research & Engineering Technology (IJSET), pp. 14–20, 2016. (in French)

[2] Djeriou, S. "Performance improvement of photovoltaic pumping system", PhD Thesis, Université M'hamed Bougara de Boumerdès, 2018. [online] Available at: https://www.ccdz.cerist.dz/admin/notice.php?id=000000000000000870000000621 [Accessed: 10 March 2022]

[3] Singh, B., Kumar, R. "Simple brushless DC motor drive for solar photovoltaic array fed water pumping system", IET Power Electronics, 9(7), pp. 1487–1495, 2016. https://doi.org/10.1049/iet-pel.2015.0852

[4] Dubey, M., Sharma, S. K., Saxena, R. "Solarpower-drivenposition sensorless control of permanent magnet brushlessDCmotor for refrigeration plant", International Transactions on Electrical Energy Systems, 30(7), e12408, 2020. https://doi.org/10.1002/2050-7038.12408/V2/DECISION1

[5] Hebib, A., Allaoui, T., Chaker, A., Belabbas, B., Denai, M. "A Comparative Study of Classical and Advanced MPPT Control Algorithms for Photovoltaic Systems", Przegląd Elektrotechniczny, 96(11), pp. 65–69, 2020. https://doi.org/10.15199/48.2020.11.14

[6] Zarour, L., Abed, K., Hacil, M., Borni, A. "Control and optimisation of photovoltaic water pumping system using sliding mode", Bulletin of the Polish Academy of Sciences Technical Sciences, 67(3), pp. 605–611, 2019. https://doi.org/10.24425/bpasts.2019.129658

[7] Rekioua, D., Achour, A. Y., Rekioua, T. "Tracking Power Photovoltaic System with Sliding Mode Control Strategy", Energy Procedia, 36, pp. 219–230, 2013. https://doi.org/10.1016/j.egypro.2013.07.025

[8] Abderrahim, T., Abdelwahed, T., Radouane, M. "Improved strategy of an MPPT based on the sliding mode control for a PV system", International Journal of Electrical and Computer Engineering (IJECE), 10(3), pp. 3074–3085, 2020. https://doi.org/10.11591/ijece.v10i3.pp3074-3085

[9] Hasan, M., Alhazmi, W. H., Zakri, W. "A fuzzy rule based control algorithm for MPPT to drive the brushless dc motor based water pump", Journal of Intelligent & Fuzzy Systems, 42(2), pp. 1003–1014, 2022. https://doi.org/10.3233/JIFS-189767

[10] Alves, D. G., Pinto, M. F., Damasceno, A. P. A. B., de Fátima Grah, V., Botrel, T. A. "Cost Analysis of Water Pumping Using Solar Energy and Diesel In Drip Irrigation", Irriga - Edição Especial Inovagri, 1(1), pp. 125–133, 2014. https://doi.org/10.15809/irriga.2014v1n1p125

[11] Sharma, R., Sharma, S., Tiwari, S. "Design optimization of solar PV water pumping system", Materials Today: Proceedings, 21(3), pp. 1673–1679, 2020. https://doi.org/10.1016/j.matpr.2019.11.322

[12] Abdelkader, H., Mohammed, Y. "Solar system design for water pumping", E3S Web of Conferences, 37, 06001, 2018. https://doi.org/10.1051/e3sconf/20183706001

[13] Arab, A. H., Benghanem, M., Gharbi, A. "Dimensionnement de Systèmes de Pompage Photovoltaïque" (Sizing of Photovoltaic Pumping Systems), Revue des Énergies Renouvelables, 8, pp. 19–26, 2005. [online] Available at: https://www.cder.dz/download/Art8-1_2.pdf [Accessed: 10 March 2022] (in French)

[14] Kashif, M., Murshid, S., Singh, B. "Standalone solar PV array fed SMC based PMSM driven water pumping system", In: 2018 IEEMA Engineer Infinite Conference (eTechNxT), New Delhi, India, 2018, pp. 1–6. ISBN 978-1-5386-1139-5 https://doi.org/10.1109/ETECHNXT.2018.8385371

[15] Jones, W. V. "Motor Selection Made Easy: Choosing the Right Motor for Centrifugal Pump Applications", IEEE Industry Applications Magazine, 19(6), pp. 36–45, 2013. https://doi.org/10.1109/MIAS.2012.2215649

[16] Aouchiche, N., Aït Cheikh, M. S., Malek, A. "Poursuite du point de puissance maximale d'un système photovoltaïque par les méthodes de l'incrémentation de conductance et la perturbation & observation" (Maximum power point tracking of a photovoltaic system by the methods of conductance incrementation and perturb & observation), Journal of Renewable Energies, 16(3), pp. 485–498, 2013. (in French) https://doi.org/10.54966/jreen.v16i3.393

[17] Salah, C. B., Ouali, M. "Comparison of fuzzy logic and neural network in maximum power point tracker for PV systems", Electric Power Systems Research, 81(1), pp. 43–50, 2011. https://doi.org/10.1016/j.epsr.2010.07.005

[18] Khireddine, M. S., Makhloufi, M. T., Abdessemed, Y., Boutarfa, A. "Tracking power photovoltaic system with a fuzzy logic control strategy", In: 2014 6th International Conference on Computer Science and Information Technology (CSIT), Amman, Jordan, 2014, pp. 42–49. ISBN 978-1-4799-3998-5 https://doi.org/10.1109/CSIT.2014.6805977

[19] Chaithanakulwat, A. "Track the maximum power of a photovoltaic to control a cascade five-level inverter a single-phase grid-connected with a fuzzy logic control", International Journal of Power Electronics and Drive Systems (IJPEDS), 10(4), pp. 1863–1874, 2019. https://doi.org/10.11591/ijpeds.v10.i4.pp1863-1874

[20] Singh, B., Bist, V. "A BL-CSC Converter-Fed BLDC Motor Drive With Power Factor Correction", IEEE Transactions on Industrial Electronics, 62(1), pp. 172–183, 2015. https://doi.org/10.1109/TIE.2014.2327551

[21] Bist, V., Singh, B. "Reduced sensor configuration of brushless DC motor drive using a power factor correction-based modified-zeta converter", IET Power Electronics, 7(9), pp. 2322–2335, 2014. https://doi.org/10.1049/iet-pel.2013.0177

[22] Mostefai, M., Miloud, Y., Miloudi, A. "One year collected and Analyzed Data in the Sahara Solar Energy Research Center in Saida, Algeria", In: 5th Asia-Africa Sustainable Energy Forum Jointly with the 7th International SSB Workshop, Tsukuba, Japan, 2015.

## Appendix

The parameters of Brushless Direct Current Motor used in the PVPS are [2]:

- rated speed ($N_{rated}$ = 2500 rpm),
- pair pole ($P$ = 2),
- stator resistance ($R_s$ = 2.875 Ω),
- stator inductance ($L_s$ = 8.5 mH),
- torque constant ($K_t$ = 1.4 Nm/A),
- voltage constant ($K_e$ = 146.6077 VL–L/krpm).

**Table A1** The boost parameters

| Parameters | Values |
|---|---|
| PV array voltage ($V_{pv}$) | 150V |
| DC link voltage ($V_{DC}$) | 360 V |
| Switching frequency ($f$) | 10 Khz |
| The boost convert duty ratio ($D$) | 0.583 |
| Inductance ($L$) | 14 mH |
| Capacitance ($C$) | 467μF |